Glutamate receptor ionotropic, kainate 1 serves as a novel tumor suppressor of colorectal carcinoma and predicts clinical prognosis

ZHONG REN*, JINGZHENG LIU*, LIQING YAO, JIAN LI, ZHIPENG QI and BING LI

Endoscopy Research Institute, Endoscopy Center, Zhongshan Hospital, Fudan University, Shanghai 200032, P.R. China

Received January 4, 2020; Accepted July 10, 2020

DOI: 10.3892/etm.2020.9296

Abstract. Colorectal cancer (CRC) is one of the most malignant cancers worldwide. However, the mechanisms of initiation and development of CRC are still largely unclear. The present study aimed to investigate the biological function and prognosis of glutamate receptor ionotropic, kainate 1 (GRIK1) in CRC. GRIK1 expression levels were analyzed in tissue microarrays containing 80 primary CRC samples using immunohistochemistry (IHC). The association between GRIK1 expression levels, clinicopathological factors and the prognosis was also investigated using Spearman's correlation analysis and Kaplan-Meier analysis, respectively. After genetic knockdown or overexpression of GRIK1, invasion/migration assays, proliferation assay, soft agar/colony formation assays, western blotting, reverse transcription-quantitative PCR and tumor xenograft models were used to investigate the function of GRIK1 both *in vitro* in two CRC cell lines, HCT116 and SW620, and *in vivo*. The results revealed that the expression levels of GRIK1 were significantly downregulated in CRC samples. Furthermore, IHC analysis indicated that the downregulated expression levels of GRIK1 were significantly associated with lymph node status and tumor size. In addition, patients with CRC with low GRIK1 expression levels demonstrated a consistently poor overall survival. The overexpression of GRIK1 inhibited the proliferation, colony formation, migration, invasion and epithelial-mesenchymal transition of HCT116 cells *in vitro*. In contrast, the genetic knockdown of GRIK1 promoted the proliferative, colony forming, migratory and invasive abilities of SW620 cells *in vitro*. Moreover, the overexpression of GRIK1 inhibited tumor growth, and liver and lung metastasis of CRC *in vivo*. In conclusion, the findings of the present study suggested that GRIK1 may serve as a tumor suppressor in CRC, and upregulated expression levels of GRIK1 may predict an improved prognosis for patients with CRC.

Correspondence to: Dr Liqing Yao, Endoscopy Research Institute, Endoscopy Center, Zhongshan Hospital, Fudan University, Building 20, 180 Fenglin Road, Shanghai 200032, P.R. China
E-mail: yaoliqingzs@yeah.net

*Contributed equally

Key words: CRC, GRIK1, tumor suppressor, metastasis, prognosis

Introduction

Colorectal cancer (CRC) is the third most commonly occurring cancer in men and the second most common cancer in women. In total, >1.8 million new cases were diagnosed in 2018 (1). Although patients with CRC can be successfully cured by undergoing curative resection when diagnosed at the early stage, 20-45% of patients still develop recurrence or metastasis (2). In fact, the 1-year survival rate of patients with CRC remains at ~36% (3). Numerous previous studies have suggested the possible mechanisms of CRC progression, such as the impact of circulating eosinophils and basophils, olfactomedin 1 and microRNA-497 on progression of CRC (4-6); however, these findings do not comprehensively explain the mechanisms behind the tumor progression and the effective treatment of this malignancy. Therefore, further investigations to determine the underlying mechanisms of the initiation and development of CRC are required.

The local colonic environment and genetic alterations may be associated with the pathogenesis of CRC. For example, *Fusobacterium nucleatum* was reported to promote CRC development in mice by upregulating the expression levels of microRNA-21, indicating that bacteria may participate in human CRC progression (7). In addition, multiple genetic and epigenetic events have been identified to stimulate the initiation, progression and metastasis of CRC in patients, including the hypermutation of BRAF (V600E), somatic copy number alterations and microsatellite alterations (8,9). Multiple studies have frequently observed the BRAF (V600E) mutation in CRC tissues, where it was discovered to predict the prognosis and drug responsiveness for patients with CRC (10,11). Furthermore, chromosomal instability has been illustrated to result in copy number alterations in patients with CRC, including losses at 1p36, 1p12, 1q21, 9p13, 14q11, 16p13 and 16p12, and gains at 7q11 and 7q22 (12). Microsatellite alterations with allelic loss at 9p24.2 were also discovered to be associated with the less aggressive metastasis of CRC (13). However, the identification of tumor suppressor genes in CRC is lacking. It has been reported that SMAD4 expression was frequently lost in CRC, and that alterations in bone morphogenetic protein signaling promoted the switch from its tumor suppressive properties to promoting metastasis (14). Notably, the adenomatous polyposis

coli (APC) tumor suppressor is mutated in ~80-90% of human CRCs, and the restoration of full-length APC was discovered to sufficiently promote cellular differentiation and inhibit CRC progression (15). However, to the best of our knowledge, the present study was the first to identify glutamate receptor ionotropic, kainate 1 (GRIK1) as a novel tumor suppressor in CRC and investigated its function both *in vitro* and *in vivo*.

Materials and methods

Clinical samples. The study was approved by the Research Ethics Committee of Zhongshan Hospital, Fudan University (Shanghai, China) and written, informed consent was obtained from all patients. All specimens were handled and anonymized according to the ethical standards of Fudan University.

CRC and adjacent normal colon tissues from 50 patients (age range, 38-74 years; 16 females and 34 males) undergoing resection for primary CRC at Zhongshan Hospital, Fudan University between May 2002 and July 2005 were used in the present study. Adjacent normal tissue was dissected from the proximal tumour resection margin with a minimum distance of 10 cm to the tumour lesion. Tissues from 80 patients (age, 22-87 years; 33 females and 47 males) with CRC who underwent curative resection between January 2002 and February 2005 at Zhongshan Hospital, Fudan University were used for tissue microarrays (TMAs) construction and prognostic analysis. The patients had not received neoadjuvant therapy prior to surgery and patients who had no follow-up information were not included in the study. The TNM stage of the patients with CRC was defined according to the 6th edition of the TNM staging system of the American Joint Committee on Cancer/International Union Against Cancer (16).

Immunohistochemistry (IHC). IHC analysis of GRIK1, proliferating cell nuclear antigen (PCNA) and cleaved caspase-3 expression levels in clinical samples was performed. Formalin-fixed, paraffin embedded specimens of tumor and adjacent normal tissues were cut into 3 μm thick sections. Slides were heated for 20 h at 37˚C. The tissue sections were deparaffinized in xylene (3 times, 5 sec each) and dehydrated via immersion in graded dilutions of alcohol solutions (absolute, 80%, 60% and water). Subsequently, the samples were boiled in citrate buffer (pH 6.0) in a microwave oven at 100˚C for 20 sec. To block endogenous peroxidase activity, the sections were treated with 3% H_2O_2 for 15 sec at room temperature. Subsequently, the sections were incubated with either an anti-GRIK1 (1:80; cat. no. 25779-1-AP; ProteinTech Group, Inc.), anti-PCNA (1:100; cat. no. ab19166; Abcam) or an anti-cleaved caspase-3 (1:100; cat. no. ab2302) primary antibody overnight at 4˚C, which was followed by incubation with horseradish peroxidase-labeled secondary antibody (1:150; cat. no. ab6721; Abcam) for 1.5 h at 37˚C. Stained cells were visualized in three randomly selected fields using a light microscope (magnification, x100, x200 or x400) and the mean Integrated Optical Density value was obtained using Image-Pro Plus version 6.0 software (Media Cybernetics, Inc.). Semi-quantitative scores of GRIK1 expression levels (negative, weak, moderate or strong staining) were used to analyze the immunostaining of each CRC sample in the TMA. The IHC staining was scored as follows: Negative (0-5% staining), weak (6-25% staining), moderate (26-50% staining) and strong (>51% staining) (17).

Cell culture. The human CRC cell lines HCT116, SW480 and SW620 were purchased from the American Type Culture Collection. All cell lines were cultured in RPMI-1640 medium (Gibco; Thermo Fisher Scientific, Inc.), supplemented with 10% FBS (Invitrogen; Thermo Fisher Scientific, Inc.), 100 U/ml penicillin and 100 g/ml streptomycin, and maintained at 37˚C in a 5% CO_2 humidified atmosphere.

Construction of GRIK1 overexpressing or short hairpin RNA (shRNA/sh) knockdown cell lines. The GRIK1 open reading frame sequence (accession no. NM_000830.4) was constructed and cloned into a lentiviral expression vector pWPXL (Addgene). The recombinant vector (5 μg) was co-transfected into 293T cells ($5x10^6$) alongside packaging plasmid psPAX2 (Addgene) and envelope plasmid pMD2.G (Addgene) using Lipofectamine® 2000 reagent (Invitrogen; Thermo Fisher Scientific, Inc.). The empty pWPXL vector was used as a control for the infection. Following 48 h after the transfection at 37˚C, the 293T lentiviral supernatant was harvested using a 0.45 μm filter, and subsequently infected into HCT116 cells (60 mm cell culture dish; $2x10^6$ cells) in the presence of 2 μg/ml polybrene (Sigma-Aldrich; Merck KGaA). Subsequent experiments were performed 2 days following infection.

shRNAs targeting GRIK1 were synthesized and cloned into the shRNA expression vector pGreenPuro (System Biosciences, LLC). The shRNA with a non-targeting sequence was used as the negative control (NC; shNC). Lentiviruses were produced in 293T cells via co-transfection of shNC, shGRIK1#1 or shGRIK1#2 (all 5 μg) with the packaging plasmid psPAX2 and envelope plasmid pMD2.G (Addgene) using Lipofectamine® 2000 (Invitrogen; Thermo Fisher Scientific, Inc.). Firstly, 293T cells ($1x10^6$) were seeded onto six-well plates in 2 ml of DMEM medium (Gibco; Thermo Fisher Scientific, Inc.) supplemented with 10% FBS and 5 μg/ml polybrene and incubated at 37˚C for 1 h. Subsequently, the medium was removed and 2 ml of fresh DMEM medium supplemented with 10% FBS were added. Viruses were harvested at 48 h after transfection, and the viral titers were determined using One-Wash Lentivirus Titer kit (OriGene Technologies, Inc.). Subsequently, SW620 cells ($1x10^6$ cells; 60 mm cell culture dish) were infected with $1x10^6$ recombinant lentivirus-transducing units in the presence of 5 μg/ml polybrene (Sigma-Aldrich; Merck KGaA). The sequences for the shRNAs used were as follows: shGRIK1#1 sense, 5'-GATCCCTGGAGCTCATCAGGCTTGCTCAGAGCCCCTGCACCAACTCACCCTGTACTTTTG-3' and antisense, 5'-AATTCAAAAGTACAGGGTGAGTTGGTGCAGGGGCTCTGAGCAAGCCTGATGAGCTCCAGGGATCG-3'; shGRIK1#2 sense, 5'-GATCCGTGCAGTCTATTTGCAATGCTCTCGAAGTTCCACACATACAGACCCGCTGTTTTG-3' and antisense, 5'-AATTCAAAACAGCGGGTCTGTATGTGTGGAACTTCGAGAGCATTGCAAATAGACTGCACG-3'; and shNC sense, 5'-GATCCCCTTCTCCGAACGTGTCACGTTTCAAGAGAACGTGACACGTTCGGAGAATTTT-3' and antisense, 5'-AGCTAAAAATTCTCCGAACGTGTCACGTTCTCTTGAAACGTGACACGTTCGGAGAAGGG-3'.

Reverse transcription-quantitative PCR (RT-qPCR). Total RNA was extracted from HCT116 and SW620 cells and tissues from patients with CRC using TRIzol® reagent (Invitrogen; Thermo Fisher Scientific, Inc.). Total RNA was reverse transcribed (37˚C for 15 min; 85˚C for 5 sec) into cDNA using a Prime-Script™ RT Reagent Kit (Takara Biotechnology Co., Ltd.) qPCR was subsequently performed to analyze the mRNA expression levels of the indicated genes using SYBR Premix Ex Taq™ II (Takara Biotechnology Co., Ltd.), according to the manufacturer's protocol, on an iCycler thermal cycler (Bio-Rad Laboratories, Inc.). The following primer pairs were used for the qPCR:GRIK1 forward, 5'-TGTCCCAGGTCAGAGT TCAC-3' and reverse, 5'-CAATCACACTTGAACTCTTTT GGT-3'; E-cadherin forward, 5'-CACCACGTACAAGGG TCAGG-3' and reverse, 5'-TCCAAGCCCTTTGCTGTT TTC-3'; N-cadherin forward, 5'-GCCAGAAAACTCCAG GGGAC-3' and reverse, 5'-TGGCCCAGTTACACGTA TCC-3'; Vimentin forward, 5'-TCCGCACATTCGAGCAAA GA-3' and reverse, 5'-TGAGGGCTCCTAGCGGTTTA-3'; Snail forward, 5'-CATAGGGCTTTGGAGTCCTGG-3' and reverse, 5'-TGAAGAGCTCGTATGGATGCC-3'; and GAPDH forward, 5'-AAGGTGAAGGTCGGAGTCAA-3' and reverse, 5'-AATGAAGGGGTCATTGATGG-3'. The relative expression levels were quantified using the $2^{-\Delta\Delta Cq}$ method ($\Delta\Delta Cq = Cq^{target\ gene}-Cq^{GAPDH}$) (18).

Western blotting. Total protein of tumor samples and cell lines was extracted using protein extraction reagent (RIPA; Thermo Fisher Scientific, Inc.) with a cocktail of proteinase inhibitors (Roche Applied Science) and a cocktail of phosphatase inhibitors (Roche Applied Science). A BCA Protein Assay kit (Pierce; Thermo Fisher Scientific, Inc.) was utilized to determine the protein concentration of the lysates. Equal amounts of total proteins (20 μg) were separated using 10% SDS-PAGE. The separated proteins were subsequently transferred onto polyvinylidene fluoride membranes (EMD Millipore) and blocked with TBS (pH 7.4) containing 8% non-fat milk and 0.1% Tween-20 at 37˚C for 1.5 h. The membranes were then incubated with the following primary antibodies overnight at 4˚C: Anti-GRIK1 (1:1,500; cat. no. 25779-1-AP; ProteinTech Group, Inc.), anti-E-cadherin: (1:1,000; cat. no. 14472; Cell Signaling Technology, Inc.), anti-N-cadherin (1:1,000; cat. no. 13116; Cell Signaling Technology, Inc.), anti-Vimentin (1:1,000; cat. no. 5741; Cell Signaling Technology, Inc.), anti-Snail (1:1,000; cat. no. 3879; Cell Signaling Technology, Inc.) and anti-GAPDH (1:2,000; cat. no. AB2302, Sigma-Aldrich; Merck KGaA). Following the primary antibody incubation, the membranes were washed with PBS-Tween-20 (0.1%) and incubated with HRP-conjugated secondary antibodies (rabbit anti-mouse HRP-conjugated IgG antibody; 1:5,000; cat. no. AP160P; and mouse anti-rabbit HRP-conjugated IgG antibody; 1:5,000, cat. no. MAB201P; both from Sigma-Aldrich; Merck KGaA) at room temperature for 2 h. Total protein was visualized using an ECL reagent (cat. no. 32106, Pierce; Thermo Fisher Scientific, Inc.) and a ChemiDoc MP Imaging System (Bio-Rad Laboratories, Inc.).

Colony formation assay. For the soft agar assay, 800 μl RPMI-1640 medium containing 0.8% sea plaque agar and 10% FBS was plated into a six-well plate and incubated at room temperature overnight. The following day, $2x10^3$/well HCT116 or SW620 cells were resuspended in adjusted 0.5% agar media (500 μl) and seeded onto the 0.8% agar plate. Following incubation at 37˚C with 5% CO^2 for 10 days, the plates were analyzed for the presence of viable colonies using a light microscope (magnification, x200).

For the plate colony formation assay, 800 HCT116 cells/well overexpressing GRIK1 or transfected with the control vector were seeded into six-well plates at 37˚C with 5% CO^2. Following incubation for 10 days, the cells were washed with PBS, fixed with 4% paraformaldehyde at room temperature for 12 h) and stained with 2% crystals violet (Sigma-Aldrich; Merck KGaA) at room temperature for 4 h). The total number of colonies containing >50 cells were counted using a light microscope (magnification, x100).

Cell proliferation assay. Cell proliferation was performed using Cell Counting Kit-8 (CCK-8) reagent (Dojindo Molecular Technologies, Inc.) according to the manufacturer's protocol. Briefly, $2x10^3$ HCT116 or SW620 cells/well were seeded into 96-well culture plates. Following incubation for 0-96 h at room temperature, 100 μl CCK-8 reagent was added to each well and incubated at 37˚C for 2 h. The absorbance was measured at a wavelength of 450 nm using a microplate reader (BioTek Instruments, Inc.).

Migration and invasion assays. A total of $2x10^5$ HCT116 or SW620 cells were plated into the upper chambers of 24-well Transwell plates (8-μm pore size; BD Biosciences) with (invasion) or without (migration) a thin layer of Matrigel (37˚C for 1 h; BD Biosciences) in RPMI-1640 medium (1% FBS). Complete RPMI-1640 medium (15% FBS) was plated into the lower chambers to act as a chemoattractant. Following incubation at 37˚C for 36 h, the invasive or migratory cells in the lower chamber were fixed with 4% paraformaldehyde at room temperature for 12 h), stained with 2% crystal violet (Sigma-Aldrich; Merck KGaA) at room temperature for 4 h, and visualized under a light microscope (magnification, x200).

Tumor growth model. Male BALB/c-nude mice (n=14; body weight, 18-20 g; age, 4 weeks; 7 mice/group) were purchased from Shanghai Laboratory Animal Center (China) and maintained in a pathogen-free animal facility with controlled temperature (25˚C) and humidity (45-55%) with alternating 12h light and dark cycle. Mice were allowed to drink and eat *ad libitum*. Mice (6-week old) were subcutaneously injected with $5x10^6$ HCT116 cells overexpressing GRIK1 or the control vector (resuspended in PBS) into the right flanks. After 4 weeks, tumors (64-1,372 mm^3) were measured with calipers and the volume was calculated using the following formula: Volume (mm^3) = [width^2 (mm^2) x length (mm)] /2. Mice were euthanized via CO_2 gas asphyxiation at an air displacement rate of 10-30% per minute at the end of experiments. To confirm the death of mice, the CO_2 flow persisted for at least 1 min after the animals had ceased breathing. Finally, tumors were dissected and weighed.

Tumor metastasis model. For the surgery, mice were anesthetized by inhalation of 2% isoflurane and were given meloxicam (2 mg/kg subcutaneously) analgesia after the

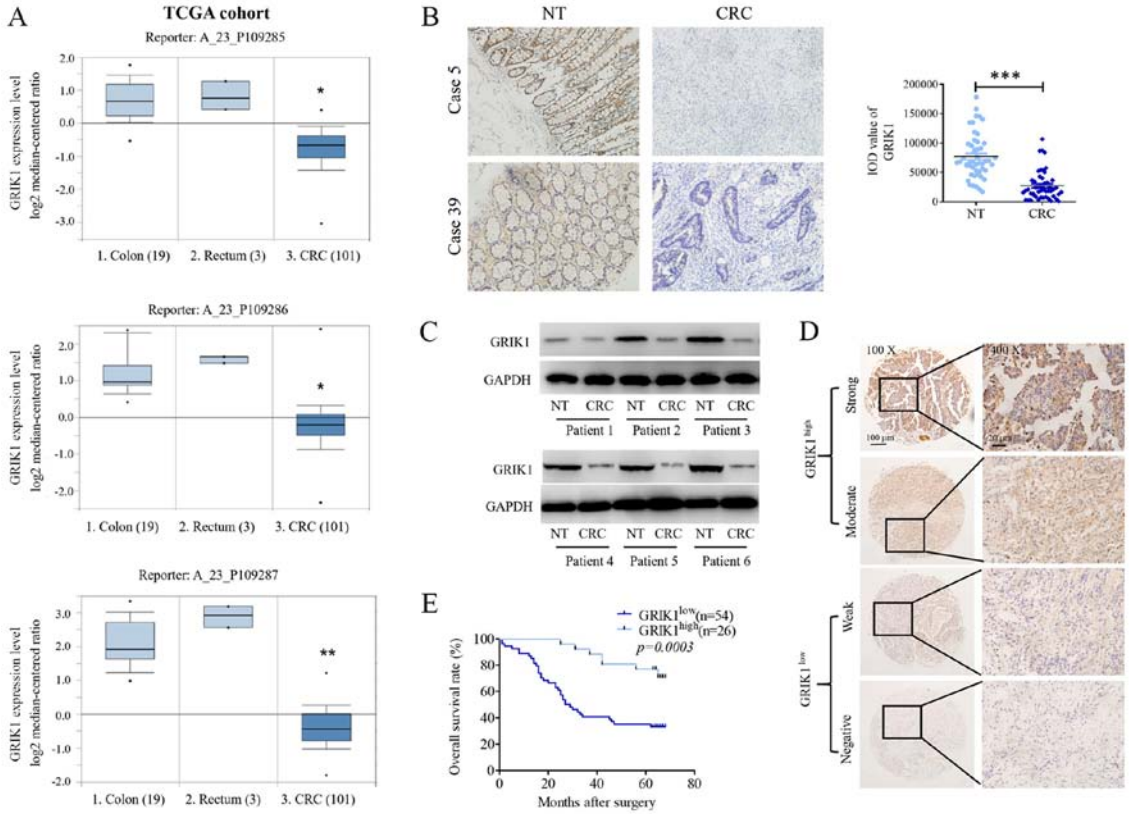

Figure 1. GRIK1 expression levels are downregulated in CRC tissues. (A) GRIK1 expression levels from TCGA dataset. Reporter probes hybridized with GRIK1: A_23_P109285; A_23_P109286; A_23_P109287). (B) Immunohistochemistry staining of GRIK1 expression levels in 50 pairs of CRC tissues and matched NT colon tissues (magnification, x100). (C) Western blotting analysis of GRIK1 expression levels in 6 pairs of CRC tissues and matched NT colon tissues. (D) GRIK1 protein expression levels were analyzed using immunohistochemistry in 80 CRC samples. Representative micrographs are shown of negative, weak, moderate and strong immunostaining of GRIK1 expression levels in CRC specimens (magnification, x100 and x400). (E) Kaplan Meier survival analysis was performed according to GRIK1 expression levels in patients with CRC. A log-rank test was used to analyze the data. GRIK1 was discovered to an independent prognostic factor for the survival of patients with CRC. *P<0.05 and **P<0.01 vs. colon or rectum tissue; ***P<0.001 vs. NT. GRIK1, glutamate receptor ionotropic, kainate 1; CRC, colorectal carcinoma; NT, non-tumorous; TCGA, The Cancer Genome Atlas; IOD, Integrated Optical Density.

surgical intervention. For the hepatic metastasis model, 16 male BALB/c-nude mice were slowly injected with $2x10^6$ HCT116 cells overexpressing GRIK1 or the control vector into the spleen, respectively. For the lung metastasis model, $2x10^6$ HCT116 cells overexpressing GRIK1 or the control vector were injected into the tail vein of male BALB/c-nude mice. After 8-10 weeks, the mice were euthanized, and the livers and lungs were collected for pathological examination. Metastatic nodules in the liver and lung tissues were analyzed using hematoxylin and eosin staining. Briefly, tissues were immersed in 4% paraformaldehyde at room temperature for 4 h and transferred to 70% ethanol. Individual biopsy material was placed in processing cassettes, dehydrated in a serial alcohol gradient, and embedded in paraffin wax blocks. Before immunostaining, 5-μm thick lung tissue sections were dewaxed in xylene, rehydrated in decreasing concentrations of ethanol, and washed in PBS. Subsequently, the sections were stained with hematoxylin and eosin (H&E Staining kit; cat no. ab245880; Abcam) at room temperature for 5 min. After staining, sections were dehydrated in increasing concentrations of ethanol and xylene, and visualized under a light microscope (magnifications, x40 and x100). All animal studies were approved by the Medical Experimental Animal Care Commission of Zhongshan Hospital, Fudan University (Shanghai, China).

Statistical analysis. The experiments were repeated at least twice. Statistical analysis was performed using SPSS 17.0 software (SPSS Inc.) and results are presented as the mean ± SD. P<0.05 was considered to indicate a statistically significant difference. Statistical differences between data with 2 groups were determined using an unpaired Student's t-test. The data with multiple groups was analyzed using one-way ANOVA followed by Tukey's post hoc test. The box and whisker plots were analyzed using a Wilcoxon signed rank test (Fig. 1B), U-Mann Whitney test (Fig. 4A, C and D) or a Kruskal-Wallis test with a Dunn's post hoc test (Fig. 1A). Kaplan-Meier analysis was used to assess survival and a log-rank test was performed to obtain the P-value. A χ^2 test was used to analyze the association between GRIK1 expression levels and the clinicopathological features of patients. Univariate analysis (log-rank test) was used to compare the survival of patients between subgroups. Multivariate analyses were performed using a multivariate Cox proportional hazard regression model.

Results

GRIK1 expression levels are downregulated in CRC tissues and predict a prognosis for patients with CRC. To investigate the role of GRIK1 in CRC progression, the expression levels of GRIK1 in tissues from The Cancer Genome Atlas

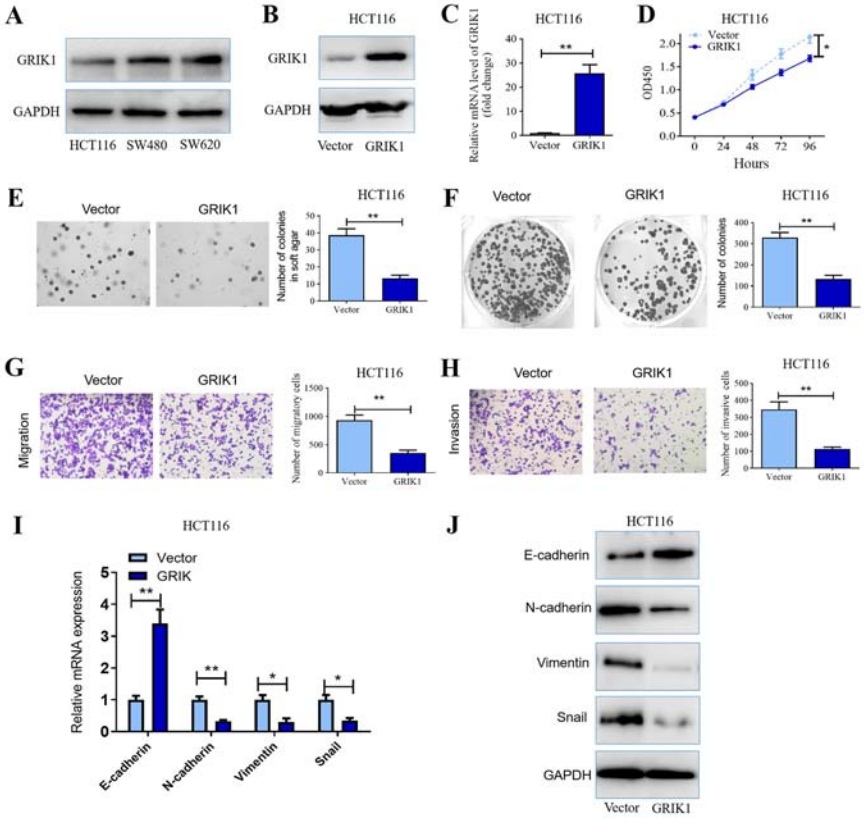

Figure 2. Overexpression of GRIK1 inhibits the proliferative, colony forming, migratory and invasive abilities of CRC cells *in vitro*. (A) GRIK1 protein expression levels in HCT116, SW480 and SW620 cell lines were determined using western blotting. Transfection efficiency of the GRIK1 overexpression vector transfected into HCT116 cells was determined using (B) western blotting and (C) RT-qPCR. (D) Cell Counting Kit-8 assay was used to determine the proliferative ability of HCT116 cells following the overexpression of GRIK1. (E) Effects of GRIK1 overexpression on the colony forming ability of HCT116 cells was analyzed using a soft agar assay (magnification, x100). (F) Plate colony formation assay was used to monitor the growth of HCT116 cells following the transfection with the GRIK1 overexpression vector. (G) Effects of GRIK1 overexpression on the migratory ability of HCT116 cells *in vitro* was determined using a Transwell assay (magnification, x400). (H) Effects of GRIK1 overexpression on the invasive ability of HCT116 cells *in vitro* was determined using a Transwell Matrigel assay (magnification, x400). (I) mRNA expression levels of EMT-related genes following the overexpression of GRIK1 were analyzed using RT-qPCR. Expression levels were normalized to the reference gene GAPDH. (J) Expression levels of EMT-related proteins following the overexpression of GRIK1 were analyzed using western blotting. *P<0.05, **P<0.01. GRIK1, glutamate receptor ionotropic, kainate 1; CRC, colorectal carcinoma; RT-qPCR, reverse transcription-quantitative PCR; EMT, epithelial-mesenchymal transition; OD, optical density.

(TCGA) database were analyzed (https://www.oncomine.org/resource/login.html; TCGA Colorectal Dataset). The results revealed that the CRC tumor tissues had markedly downregulated expression levels of GRIK1 compared with the normal colon and rectum tissues in TGGA dataset (three different reporters of GRIK1; Fig. 1A). The expression levels of GRIK1 in 50 pairs of CRC specimens (tumor and corresponding non-tumor tissues) were subsequently analyzed using IHC analysis. Similarly, the protein expression levels of GRIK1 were significantly downregulated in the CRC tissues compared with the adjacent normal tissues (Fig. 1B). Moreover, the results from the western blotting assays revealed that the expression levels of GRIK2 were downregulated in CRC tissues compared with their corresponding non-tumor tissues (Fig. 1C).

Subsequently, IHC staining was used to analyze the expression levels of GRIK1 in a TMA containing 80 CRC tissues; the intensity of GRIK1 staining was categorized into negative, weak, moderate or strong staining. Samples with negative and weak staining were defined as having low expression levels of GRIK1 (n=54), while those with moderate and strong staining were defined as having high expression levels of GRIK1 (n=26) (Fig. 1D). The relationship between GRIK1 expression levels and the clinicopathological features was determined. The results revealed that low expression levels of GRIK1 were significantly associated with lymphovascular invasion and tumor size (Table I). Kaplan-Meier survival analysis also discovered that patients with CRC with low expression levels of GRIK1 had a shorter overall survival (OS; Fig. 1E). Moreover, univariate analysis indicated that the node stage, metastasis stage, lymphovascular invasion, tumor size, tumor grade and GRIK1 expression levels were significantly associated with the OS of patients with CRC (Table II). Multivariate analysis further indicated that GRIK1 expression levels, N stage and tumor size were an independent prognostic factor for patients with CRC (Table II).

Overexpression of GRIK1 inhibits the proliferation, colony formation, migration, invasion and epithelial-mesenchymal transition (EMT) of CRC cells in vitro. The expression levels of GRIK1 were investigated in three CRC cell lines, HCT116, SW480 and SW620. Western blotting analysis revealed that HCT116 cells demonstrated relatively low expression levels of GRIK1, while in comparison, the other two cell lines

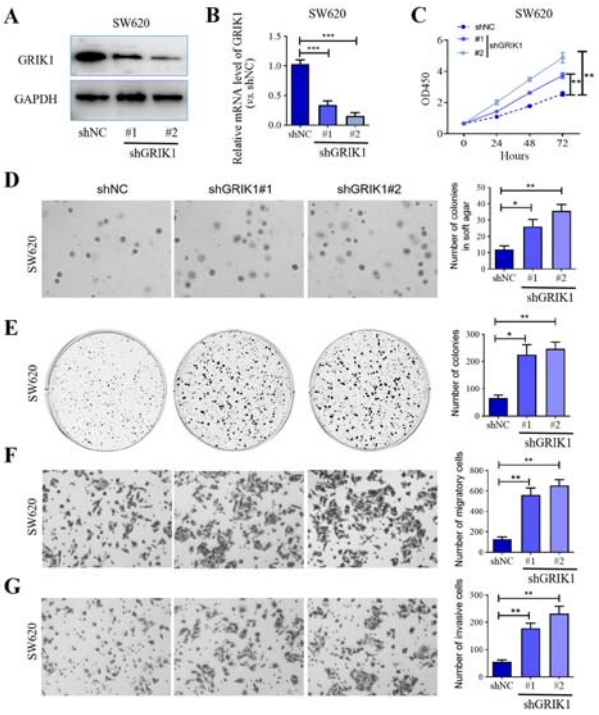

Figure 3. Knockdown of GRIK1 promotes the proliferative, colony forming, migratory and invasive abilities of colorectal carcinoma cells *in vitro*. Transfection efficiency of shGRIK1#1 and shGRIK1#2 in SW620 cells was determined using (A) western blotting and (B) reverse transcription-quantitative PCR. (C) Cell Counting Kit-8 assay was used to determine the proliferation of SW620 cells following GRIK1 knockdown. (D) Effects of GRIK1 knockdown on the colony formation of SW620 cells in soft agar assay (magnification, x100). (E) Plate colony formation assay was used to determine growth of SW620 cells following GRIK1 knockdown. (F) Effects of GRIK1 knockdown on the migratory ability of SW620 cells *in vitro* was determined using a Transwell assay (magnification, x400). (G) Effects of GRIK1 knockdown on the invasive ability of SW620 cells *in vitro* was determined using a Transwell Matrigel assay (magnification, x400). *P<0.05, **P<0.01, ***P<0.001. GRIK1, glutamate receptor ionotropic, kainate 1; sh, short hairpin RNA; NC, negative control.

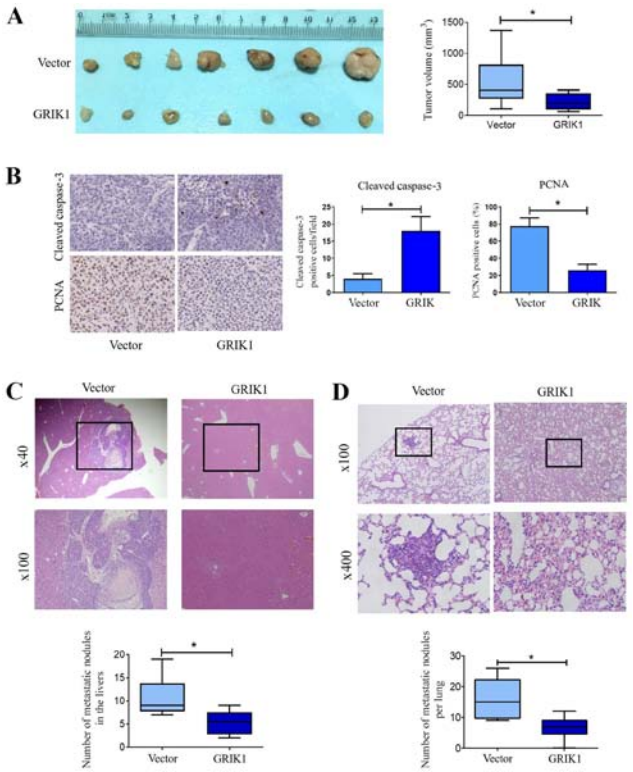

Figure 4. Overexpression of GRIK1 inhibits tumor growth and the metastasis of colorectal carcinoma *in vivo*. (A) HCT116 cells stably overexpressing GRIK1 were subcutaneously injected into the flanks of nude mice. Tumor volumes were analyzed (n=7/group). (B) Immunohistochemistry analysis of cleaved caspase-3 and PCNA expression levels in the GRIK1 and vector groups of the HCT116 xenograft model (magnification, x200). (C) Representative H&E staining micrographs of metastatic nodules in the liver from the GRIK1 overexpression and vector groups of the HCT116 xenograft model (n=8/group; magnification, x40 or x100). (D) Representative H&E staining micrographs of the metastatic nodules in the lung from GRIK1 overexpression and vector groups of the HCT116 xenograft model (n=8/group; magnification, x40 or x100). *P<0.05. GRIK1, glutamate receptor ionotropic, kainate 1; PCNA, proliferating cell nuclear antigen.

Table I. Association between GRIK1 expression levels and patient clinicopathological features.

Variable	Glutamate receptor ionotropic, kainate 1 protein expression levels		P-value
	Low	High	
Sex			0.894
Male	32	15	
Female	22	11	
Age			0.463
≤60	19	12	
>60	35	14	
T stage			0.259
T1/T2	10	8	
T3/T4	44	18	
N stage			0.162
N0	21	16	
N1	24	7	
N2	9	3	
M stage			0.125
M0	41	24	
M1	13	2	
Lymphovascular invasion			0.003
Negative	32	24	
Positive	22	2	
Tumor size, cm			0.008
≤5	21	19	
>5	33	7	
G			0.681
G1	10	6	
G2	22	12	
G3	22	8	

GRIK1, glutamate receptor ionotropic, kainate 1; T, tumor; N, node; M, metastasis; G, grade.

expressed relatively high expression levels of GRIK1 (Fig. 2A). Subsequently, the biological functions of GRIK1 *in vitro* were determined. Considering that HCT116 cells were indicated to express GRIK1 at a relative low level, GRIK1 was overexpressed in this cell line. Following the transfection of HCT116 cells with GRIK1 overexpression vectors, the expression levels of GRIK1 were discovered to be upregulated compared with the vector control-transfected cells (Fig. 2B and C). The results from the CCK-8 assay further illustrated that the overexpression of GRIK1 significantly inhibited the proliferation of HCT116 cells compared with the vector control after 72 and 96 h culture (Fig. 2D). In addition, the overexpression of GRIK1 also significantly inhibited the colony forming ability of HCT116 cells compared with the vector control (Fig. 2E and F). Similarly, the overexpression of GRIK1 significantly reduced the migratory and invasive abilities of HCT116 cells compared with the vector control (Fig. 2G and H).

Furthermore, the expression levels of EMT markers were also analyzed following the overexpression of GRIK1. The results revealed that the overexpression of GRIK1 downregulated N-cadherin, Vimentin and snail expression levels, while upregulating E-cadherin expression levels in HCT116 cells at both the mRNA and protein level compared with the vector control group (Fig. 2I and J). Taken together, these data suggested that GRIK1 may exert a tumor suppressive function in CRC cells *in vitro*.

Knockdown of GRIK1 promotes the proliferation, colony formation, migration and invasion of CRC cells in vitro. To further confirm the tumor suppressive function of GRIK1, GRIK1 was knocked down in SW620 cells, which expressed GRIK1 at a relatively high level, using two different shRNAs. Western blotting and RT-qPCR analysis confirmed that the expression levels of GRIK1 were efficiently knocked down in SW620 cells transfected with shGRIK1#1/2 compared with the shNC group (Fig. 3A and B). The results of the CCK-8 assay further illustrated that the knockdown of GRIK1 with both shGRIK1#1 and shGRIK1#2 significantly promoted the prolif-

Table II. Univariate and multivariate analysis of patient parameters.

	Univariate analysis		Multivariate analysis	
Variable	HR (95% CI)	P-value	HR (95% CI)	P-value
Sex	1.397 (0.766-2.547)	0.276		
Age	1.269 (0.670-2.403)	0.466		
Tumor stage	1.262 (0.585-2.277)	0.553		
Node stage	1.526 (1.052-2.214)	0.026	1.966 (1.237-3.126)	0.004
Metastasis stage	2.094 (1.030-4.260)	0.041		
Lymphovascular invasion	1.979 (1.060-3.694)	0.032		
Tumor size	2.943 (1.549-5.591)	0.001	3.690 (1.740-7.823)	0.001
Grade	1.479 (0957-2.285)	0.078		
Expression level of glutamate receptor ionotropic, kainate 1	0.462 (0.237-0.900)	0.001	0.251 (0.111-0.567)	0.020

HR, hazard ratio; CI, confidence interval.

eration of SW620 cells compared with the shNC group after 48 or 72 h culture (Fig. 3C). In addition, the knockdown of GRIK1 also enhanced the colony forming ability of SW620 cells compared with the shNC group (Fig. 3D and E). In contrast to the overexpression of GRIK1, the knockdown of GRIK1 significantly promoted the migratory and invasive abilities of SW620 cells compared with the shNC group (Fig. 3F and G). Taken together, these data further suggested that GRIK1 may exert tumor suppressive functions in CRC cells *in vitro*.

Overexpression of GRIK1 inhibits tumor growth and the metastasis of CRC in vivo. To investigate the role of GRIK1 *in vivo*, HCT116 cells stably overexpressing GRIK1 were subcutaneously injected into the flanks of nude mice. The results revealed that the overexpression of GRIK1 significantly inhibited tumor growth *in vivo* compared with the vector group (Fig. 4A). In addition, IHC analysis further demonstrated that the overexpression of GRIK1 significantly upregulated the expression levels of cleaved caspase-3, while downregulating those of PCNA in tumor tissues overexpressing GRIK1 compared with the vector group (Fig. 4B).

Subsequently, hepatic and lung metastases were also analyzed *in vivo*. The results demonstrated that the overexpression of GRIK1 decreased the number and size of metastatic liver (Fig. 4C) and pulmonary nodules (Fig. 4D) compared with the vector group. Collectively, these results indicated that GRIK1 may inhibit the growth and metastasis of CRC cells *in vivo*.

Discussion

It has been previously reported that individuals with Down's syndrome (trisomy 21) exhibited remarkably reduced incidence rates of a large proportion of solid tumors, including colon, pancreatic and breast cancer (19-21). It was suggested that the upregulated expression levels of 534 genes located on the extra copy of chromosome 21 (HSA21) conferred this broad cancer protection to individuals with Down's syndrome (20). These findings have provided an opportunity to identify tumor suppressor genes located on HSA21. Accumulating evidence has supported the association between HSA21 genes and the suppression of numerous types of malignant solid tumor (22-24). Previously, Jin *et al* (22) demonstrated that the HSA21 gene, calcipressin-1 isoform 4 (RCAN1.4), functioned as a novel tumor suppressor of hepatocellular carcinoma (HCC) through preventing the angiogenesis, growth and metastasis of HCC. Kuwahara *et al* (24) reported that the germinal-center associated nuclear protein encoded on HSA21 was associated with tumorigenesis and development of breast cancer. The human GRIK1 gene is a HSA21 gene, located on the q21.3 region of the chromosome (25). Similar to other HSA21 genes such as RCAN1.4, the GRIK1 gene was considered to be a strong candidate gene responsible for the Down's syndrome phenotype (26). In addition, TCGA data of HCC samples revealed that GRIK1 was one of the HSA21 genes identified to be downregulated (22). The results of the present study supported that GRIK1 may be another candidate tumor suppressor of numerous types of solid tumor. The clinical data of the present study demonstrated that the expression levels of GRIK1 were downregulated in CRC samples compared with normal colon or rectum tissues. Furthermore, the expression levels of GRIK1 were associated with lymph node status and tumor size. In addition, patients with CRC and low GRIK1 expression levels demonstrated a consistently poor overall survival rate compared with patients with CRC and high GRIK1 expression levels, indicating a possible tumor suppressive function of GRIK1 in CRC progression. Therefore, it would be worth investigating the biological function of GRIK1 in other types of solid tumor, including HCC, breast cancer or pancreatic cancer. Likewise, the tumor suppressive functions of other downregulated HSA21 genes should be investigated in future studies.

The gene product of GRIK1 belongs to the kainate family of glutamate receptors, which consist of four subunits

and function as ligand-activated ion channels (27). Allelic variants of GRIK1 were reported to contribute a major genetic determinant to the pathogenesis of juvenile absence epilepsy-related phenotypes (28). In addition, the single nucleotide polymorphism rs455804 on 21q21.3, which is located within intron 1 of GRIK1, was previously reported to be associated with hepatitis B-induced HCC (29). However, to the best of our knowledge, the biological function of GRIK1 has never been reported before. The present study demonstrated for the first time that the overexpression of GRIK1 significantly inhibited the colony forming, proliferative, migratory and invasive abilities of CRC cells. By contrast, knockdown of GRIK1 promoted theses malignant functions of CRC cells *in vitro*. In addition, GRIK1 was also associated with EMT-induced malignant transformation, which was supported by the downregulated N-cadherin, Vimentin and Snail expression, and the upregulated E-cadherin expression in HCT116 cells at both the mRNA and protein level following overexpression of GRIK1. Furthermore, *in vivo* tumor models were also used to validate the tumor suppressive function of GRIK1. As expected, the overexpression of GRIK1 potently prevented the growth and metastasis of CRC tumors *in vivo*. Moreover, IHC analysis further demonstrated that the overexpression of GRIK1 significantly upregulated the expression levels of cleaved caspase-3, while it downregulated those of PCNA in tumor tissues overexpressing GRIK1, compared with the vector group. All these results indicated that GRIK1 may act as a tumor suppressor *in vivo*. However, the limitations of the present study were the lack of mechanistic investigations and additional animal tumor models, such as the immune-competent transgenic model (30). Minbay *et al* (31) reported that homomeric or heteromeric functional receptor channels were formed through the combination of different ionotropic glutamate receptor subunits in red nucleus neurons in normal adult female Sprague-Dawley rats. Therefore, further functional and pharmacological studies should determine whether GRIK1 combines to other subunits to serve tumor suppressive functions in CRC.

On the other hand, GRIK1 is involved in glutamate signaling; several studies have reported that glutamate signaling served a central role in the malignant phenotype of numerous types of tumor, such as liver and breast cancer, via multiple molecular mechanisms, including the regulation of Snail expression or STAT3 signaling pathways (32-34). Considering these findings, the role of GRIK1 in regulating the glutamate signaling pathway in CRC should also be further investigated.

In conclusion, the findings of the present study indicated that the downregulation of GRIK1 may predict a poor prognosis for patients with CRC, which may be due to its association with malignant features of CRC, such as tumor growth, metastasis and EMT. Thus, GRIK1 was identified as a potential novel tumor suppressor in CRC and may represent a putative therapeutic target for CRC.

Acknowledgements

Not applicable.

Funding

The present study was funded by grants from the Shanghai Engineering and Research Center of Diagnostic and Therapeutic Endoscopy (grant no. 16DZ2280900) and The Project of Shanghai Science and Technology Commission: The Research of the Use of Antibiotics in POEM for Esophageal Achalasia (grant no. 16411950409)

Availability of data and materials

The datasets used and/or analyzed during the current study are available from the corresponding author on reasonable request. The datasets generated and/or analyzed during the current study are available in the Oncomine repository (https://www.oncomine.org/resource/login.html).

Authors' contributions

LY and ZR conceptualized and designed the study; ZR, JZL, JL and ZQ performed the experiments; ZQ and BL analyzed and interpreted the data; ZR and JL drafted the manuscript; and JZL and ZQ critically revised the manuscript for important intellectual content. All authors read and approved the final manuscript.

Ethics approval and consent to participate

All animal studies were approved by the Medical Experimental Animal Care Commission of Zhongshan Hospital, Fudan University (Shanghai, China). The patient studies (approval no. Y2020-145) were approved by the Research Ethics Committee of Zhongshan Hospital, Fudan University (Shanghai, China) and written, informed consent was obtained from all patients.

Patient consent for publication

Not applicable.

Competing interests

The authors declare that they have no competing interests.

References

1. Rawla P, Sunkara T and Barsouk A: Epidemiology of colorectal cancer: Incidence, mortality, survival, and risk factors. Prz Gastroenterol 14: 89-103, 2019.
2. Winawer S, Fletcher R, Rex D, Bond J, Burt R, Ferrucci J, Ganiats T, Levin T, Woolf S, Johnson D, *et al*; Gastrointestinal Consortium Panel: Colorectal cancer screening and surveillance: Clinical guidelines and rationale-Update based on new evidence. Gastroenterology 124: 544-560, 2003.
3. Rees M, Tekkis PP, Welsh FK, O'Rourke T and John TG: Evaluation of long-term survival after hepatic resection for metastatic colorectal cancer: A multifactorial model of 929 patients. Ann Surg 247: 125-135, 2008.
4. Wei Y, Zhang X, Wang G, Zhou Y, Luo M, Wang S and Hong C: The impacts of pretreatment circulating eosinophils and basophils on prognosis of stage I-III colorectal cancer. Asia Pac J Clin Oncol 14: e243-e251, 2018.
5. Shi W, Ye Z, Zhuang L, Li Y, Shuai W, Zuo Z, Mao X, Liu R, Wu J, Chen S, *et al*: Olfactomedin 1 negatively regulates NF-κB signalling and suppresses the growth and metastasis of colorectal cancer cells. J Pathol 240: 352-365, 2016.

6. Qiu YY, Hu Q, Tang QF, Feng W, Hu SJ, Liang B, Peng W and Yin PH: MicroRNA-497 and bufalin act synergistically to inhibit colorectal cancer metastasis. Tumour Biol 35: 2599-2606, 2014.
7. Yang Y, Weng W, Peng J, Hong L, Yang L, Toiyama Y, Gao R, Liu M, Yin M, Pan C, *et al*: *Fusobacterium nucleatum* increases proliferation of colorectal cancer cells and tumor development in mice by activating toll-like receptor 4 signaling to nuclear factor-κB, and up-regulating expression of microRNA-21. Gastroenterology 152: 851-866.e24, 2017.
8. Carethers JM and Jung BH: Genetics and genetic biomarkers in sporadic colorectal cancer. Gastroenterology 149: 1177-1190.e3, 2015.
9. Okugawa Y, Grady WM and Goel A: Epigenetic alterations in colorectal cancer: Emerging biomarkers. Gastroenterology 149: 1204-1225.e12, 2015.
10. Prahallad A, Sun C, Huang S, Di Nicolantonio F, Salazar R, Zecchin D, Beijersbergen RL, Bardelli A and Bernards R: Unresponsiveness of colon cancer to BRAF(V600E) inhibition through feedback activation of EGFR. Nature 483: 100-103, 2012.
11. Barras D, Missiaglia E, Wirapati P, Sieber OM, Jorissen RN, Love C, Molloy PL, Jones IT, McLaughlin S, Gibbs P, *et al*: BRAF V600E mutant colorectal cancer subtypes based on gene expression. Clin Cancer Res 23: 104-115, 2017.
12. Arriba M, García JL, Inglada-Pérez L, Rueda D, Osorio I, Rodríguez Y, Álvaro E, Sánchez R, Fernández T, Pérez J, *et al*: DNA copy number profiling reveals different patterns of chromosomal instability within colorectal cancer according to the age of onset. Mol Carcinog 55: 705-716, 2016.
13. Koi M, Garcia M, Choi C, Kim HR, Koike J, Hemmi H, Nagasaka T, Okugawa Y, Toiyama Y, Kitajima T, *et al*: Microsatellite alterations with allelic loss at 9p24.2 signify less-aggressive colorectal cancer metastasis. Gastroenterology 150: 944-955, 2016.
14. Voorneveld PW, Kodach LL, Jacobs RJ, Liv N, Zonnevylle AC, Hoogenboom JP, Biemond I, Verspaget HW, Hommes DW, de Rooij K, *et al*: Loss of SMAD4 alters BMP signaling to promote colorectal cancer cell metastasis via activation of Rho and ROCK. Gastroenterology 147: 196-208.e13, 2014.
15. Dow LE, O'Rourke KP, Simon J, Tschaharganeh DF, van Es JH, Clevers H and Lowe SW: Apc restoration promotes cellular differentiation and reestablishes crypt homeostasis in colorectal cancer. Cell 161: 1539-1552, 2015.
16. Li X, Chen T, Shi Q, Li J, Cai S, Zhou P, Zhong Y and Yao L: Angiopoietin-like 4 enhances metastasis and inhibits apoptosis via inducing bone morphogenetic protein 7 in colorectal cancer cells. Biochem Biophys Res Commun 467: 128-134, 2015.
17. Yang C, Wang S, Ruan H, Li B, Cheng Z, He J, Zuo Q, Yu C, Wang H, Lv Y, *et al*: Downregulation of PDK4 increases lipogenesis and associates with poor prognosis in hepatocellular carcinoma. J Cancer 10: 918-926, 2019.
18. Livak KJ and Schmittgen TD: Analysis of relative gene expression data using real-time quantitative PCR and the 2(-Δ Δ C(T)) method. Methods 25: 402-408, 2001.
19. Hasle H, Clemmensen IH and Mikkelsen M: Risks of leukaemia and solid tumours in individuals with Down syndrome. Lancet 355: 165-169, 2000.
20. Hasle H, Friedman JM, Olsen JH and Rasmussen SA: Low risk of solid tumors in persons with Down syndrome. Genet Med 18: 1151-1157, 2016.
21. Pussegoda KA: Down syndrome patients are less likely to develop cancer. Clin Genet 78: 35-37, 2010.
22. Jin H, Wang C, Jin G, Ruan H, Gu D, Wei L, Wang H, Wang N, Arunachalam E, Zhang Y, *et al*: Regulator of calcineurin 1 gene isoform 4, down-regulated in hepatocellular carcinoma, prevents proliferation, migration, and invasive activity of cancer cells and metastasis of orthotopic tumors by inhibiting nuclear translocation of NFAT1. Gastroenterology 153: 799-811.e33, 2017.
23. Dey N, Krie A, Klein J, Williams K, McMillan A, Elsey R, Sun Y, Williams C, De P and Leyland-Jones B: Down syndrome and triple negative breast cancer: A rare occurrence of distinctive clinical relationship. Int J Mol Sci 18: E1218, 2017.
24. Kuwahara K, Yamamoto-Ibusuki M, Zhang Z, Phimsen S, Gondo N, Yamashita H, Takeo T, Nakagata N, Yamashita D, Fukushima Y, *et al*: GANP protein encoded on human chromosome 21/mouse chromosome 10 is associated with resistance to mammary tumor development. Cancer Sci 107: 469-477, 2016.
25. Hattori M, Fujiyama A, Taylor TD, Watanabe H, Yada T, Park HS, Toyoda A, Ishii K, Totoki Y, Choi DK, *et al*; Chromosome 21 mapping and sequencing consortium: The DNA sequence of human chromosome 21. Nature 405: 311-319, 2000.
26. Li W, Wang X and Li S: Investigation of copy number variations on chromosome 21 detected by comparative genomic hybridization (CGH) microarray in patients with congenital anomalies. Mol Cytogenet 11: 42, 2018.
27. Barbon A and Barlati S: Genomic organization, proposed alternative splicing mechanisms, and RNA editing structure of GRIK1. Cytogenet Cell Genet 88: 236-239, 2000.
28. Sander T, Hildmann T, Kretz R, Fürst R, Sailer U, Bauer G, Schmitz B, Beck-Mannagetta G, Wienker TF and Janz D: Allelic association of juvenile absence epilepsy with a GluR5 kainate receptor gene (GRIK1) polymorphism. Am J Med Genet 74: 416-421, 1997.
29. Matsuda K: Novel susceptibility loci for hepatocellular carcinoma in chronic HBV carriers. Hepatobiliary Surg Nutr 1: 59-60, 2012.
30. Luo Y, Xie C, Brocker CN, Fan J, Wu X, Feng L, Wang Q, Zhao J, Lu D, Tandon M, *et al*: Intestinal PPARα protects against colon carcinogenesis via regulation of methyltransferases DNMT1 and PRMT6. Gastroenterology 157: 744-759.e4, 2019.
31. Minbay Z, Serter Kocoglu S, Gok Yurtseven D and Eyigor O: Immunohistochemical localization of ionotropic glutamate receptors in the rat red nucleus. Bosn J Basic Med Sci 17: 29-37, 2017.
32. Kuo TC, Chen CK, Hua KT, Yu P, Lee WJ, Chen MW, Jeng YM, Chien MH, Kuo KT, Hsiao M, *et al*: Glutaminase 2 stabilizes Dicer to repress Snail and metastasis in hepatocellular carcinoma cells. Cancer Lett 383: 282-294, 2016.
33. Cacace A, Sboarina M, Vazeille T and Sonveaux P: Glutamine activates STAT3 to control cancer cell proliferation independently of glutamine metabolism. Oncogene 36: 2074-2084, 2017.
34. Christa L, Simon MT, Flinois JP, Gebhardt R, Brechot C and Lasserre C: Overexpression of glutamine synthetase in human primary liver cancer. Gastroenterology 106: 1312-1320, 1994.